Krajowa Konferencja Zastosowań Matematyki w Biologii i Medycynie

Jastrzębia Góra, 16th–20th September 2013

ON THE NECESSITY OF EXPERIMENTAL VERIFICATION OF NUMERICAL RESULTS IN BIOMEDICAL APPLICATIONS

Grzegorz Rotta[1] **and Tomasz Seramak**[2]

[1]Machine Design and Vehicles Department, Gdańsk University of Technology,
ul. Narutowicza 11/12, 80-233, Gdańsk
[2]Department of Material Engineering and Welding, Gdańsk University of Technology,
ul. Narutowicza 11/12, 80-233, Gdańsk
[1]grotta@pg.gda.pl, [2]tseramak@pg.gda.pl

ABSTRACT

Porous structures made of metal or biopolymers with a structure similar in shape and mechanical properties to human bone can be easily produced by stereolitography techniques, *e.g.* selective laser melting (SLM). Numerical techniques, like finite element method (FEM) have great potential in testing new, even the most sophisticated designs, according to their mechanical properties, *i.e.* strength or stiffness. However, due to different types of elements and varying mesh density of the model, numerical results can vary over a wide range. Experimental verification would be helpful for adjusting optimal mesh density and selecting proper element type, in order to obtain reliable results connected with reasonable solution time. This paper shows variability of results regarding to mesh density, and element types.

INTRODUCTION

Tissue engineering is a branch of biomedical science known for combining living tissue and engineered materials. Titanium and its alloys are a top as the material of choice biomedical applications due to their excellent mechanical properties, biocompatibility and chemical stability. However, main drawback for their clinical applications is the difference between mechanical properties of the bulk titanium and natural bones, which causes stress shielding, bone atrophy and eventually implant loosening. Recently, many researchers have devoted notable efforts to prepare methodology of design and manufacturing porous structures, that have mechanical properties similar to bone (especially stiffness and Young modulus). Porosity also provides proper environment for bone ingrowth in order to achieve a good fixation between porous implant and the surrounding bone. Nowadays, there are a number of manufacturing techniques for the fabrication of porous structures (both for metal and nonmetal materials): selective laser melting (SLM) [1–4] selective laser sintering (SLS) techniques [5], powder metallurgy (PM) [5, 6], freeze casting [7], space holder [8], sponge replication [9]. These methods are applicable to other biomedical materials like stainless steels, biopolymers or ceramics as well [2, 9].

Selective laser melting (SLM) technique involves a high precision scanning layer–by–layer and solidification of metal powder in layers sectioned directly from a computer–aided design (CAD) model [1, 2, 10]. High energy laser is used to selectively fusing thin powder layers, therefore this method has the ability to manufacture sophisticated and complex engineering structures that could

not be made by conventional techniques i.e casting or machining. Combination of SLM and CAD techniques makes custom implant design by possible producing individual, predesigned scaffolds with predefined macro- and microstructures for hard tissue engineering [3]. Example of porous scaffold made of stainless steel 316L and designed by Authors is presented in Fig. 1.

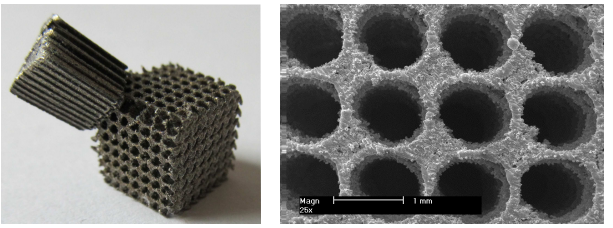

Figure 1. Porous structure with cylindrical pores made at the laboratory of Department of Material Engineering and Welding (Gdańsk University of Technology).

New scaffold architecture, can be designed with the use of numerical methods *e.g.* by finite element method, before SLM processing. Stiffness or Young modulus of designed structure, can be estimated through the calculated strains or displacements, whilst strength of the scaffold through the maximum stress. However, in the finite element method, there are a lot of specific factors, like different techniques of three dimensional modeling (Fig. 2), various types of boundary conditions (*i.e.* load expressed as force or pressure, symmetry *etc.*), and elements, which are available in a number of configurations (low or high order *i.e.* with or without midside nodes, tetrahedral, pyramids, wedges, or hexahedral *i.e.* bricks element shapes; with or without rotational degrees of freedom) [11].

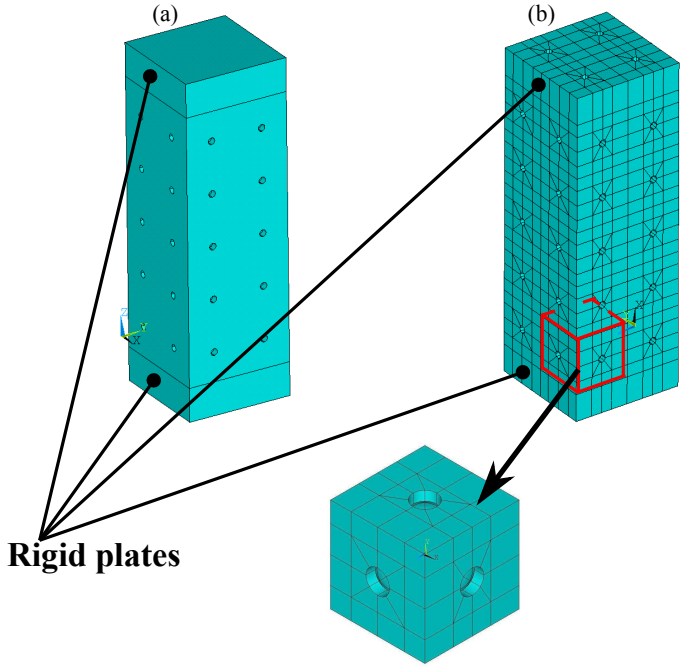

Figure 2. Two ways of making general geometry for MES models: (a) one volume designed by CAD systems—only for free meshing; (b) multi–volume model designed by APDL (Ansys Parametric Design Language)—all the volumes are hexahedrons—for free– or mapped– meshing.

All of these factors may have an effect on calculated results. Moreover, total number of elements, *i.e.* mesh density strongly affects results as well. Thus, there is the necessity for experimental verification of the numerical model created for new proposed scaffold or porosity material design. Especially when atypical configuration or shapes of cells are made, and when wide scope of different configurations, based on new design are planned, experimental investigation is indispensable.

NUMERICAL ANALYSIS: GEOMETRICAL MODEL, MESH GRID AND BOUNDARY CONDITIONS

Finite element simulations were carried out using ANSYS 13.0 environment. A three–dimensional finite element model of a regular structured scaffolds was used. A single cell of investigated scaffold is a cube the size of 0.778mm$\times$0.778mm$\times$0.778mm, with a spherical void 0.6 mm diameter at the center, and channels 0.1mm in diameter on each side of the cube. Porosity of the scaffold is 75%. Total dimensions of the modeled porous structure was 1.556$\times$1.556$\times$3.89 mm (2$\times$2$\times$5 pores—Fig. 2). Three types of 3D structural solid elements were used: 8–node Structural SOLID185, 20–node Structural SOLID186 and 10–node Tetrahedral Structural SOLID187. All of them are suitable for modeling general 3–D solid structures, however, the last two are recommended for modeling irregular meshes, such as those produced by various CAD/CAM systems. Basically, two types of mesh grid are allowed: mapped mesh (only for SOLID's 185 and 186), also known as a "brick" mesh, when all the elements are hexahedral (Fig. 3(b)), and free mesh, when elements are tetrahedral (Fig. 3(b)). A mapped mesh is possible only if the geometry is designed in APDL (Ansys Parametric Design Language).

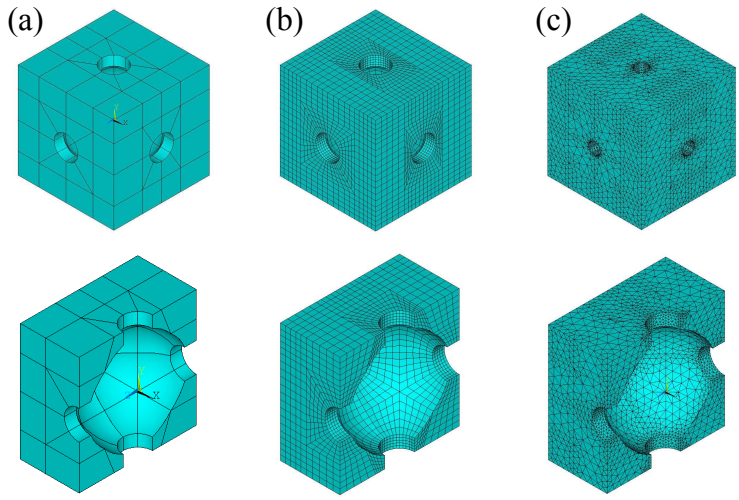

Figure 3. Comparison of mapped mesh and free mesh: (a) component hexahedral volumes of one elemental cell, (b) mapped meshing—29744 nodes, 20736 elements; (c) free meshing—34161 nodes, 138734 elements. Low order element SOLID185 in all cases.

It should be noticed, that free meshing always generates more elements and nodes than mapped meshing, so the computational effort in this case is larger than in a model with brick elements, *e.g.* one elemental cell mapped meshing generates 29744 nodes and 20736 elements, whilst free meshing—34161 nodes, 138734 elements—under the assumption more or less comparable element size in both cases—see Fig. 3. On the contrary, Fig. 4 shows comparison of element size for different mesh grids.

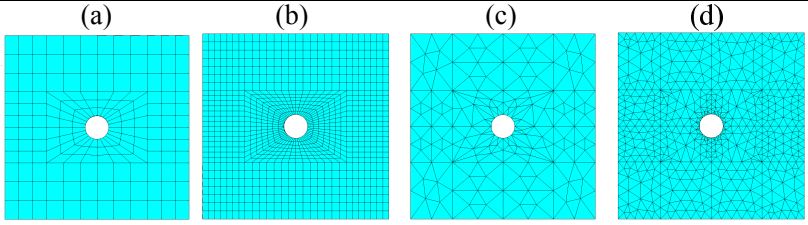

Figure 4. Comparison of mesh grids: (a) mapped mesh 50 000 elements, (b) mapped mesh 620 000 elements, (c) free mesh 189 000 elements, d) free mesh 1 150 00 elements.

A stretch force of 1000N was applied to one end of the model, whilst the other end was constrained (Fig. 5). Force was applied through rigid plate, thus nodal force would not influence directly on the scaffold boundary. Calculation time is strongly dependent on a mesh density and an element type and varied from several minutes to 6 hours on computer with 2 DualCore AMD Opteron 275 processors and 12 GB RAM memory.

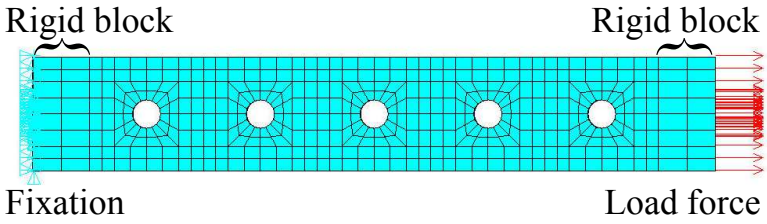

Figure 5. Boundary conditions (only one row of elemental cells is shown, mesh density is artificially lowered for better clarity of the picture).

NUMERICAL ANALYSIS: RESULTS AND DISCUSSION

Figures 6 and 7 show typical contours of stresses; they are very similar in all cases considered, just values of stresses or displacements are varied with the element types and shapes or mesh grid. A set of results for different element types and shapes or mesh grid are in Table 1 and Fig. 8. There are large differences between calculated stresses for both types of elements; element type SOLID185 gives more or less 100–130 MPa lower stresses than SOLID186 and SOLID187. Maximum values appear in places where spheres connect with cylindrical channels interconnected neighbouring spheres, and this is due to a different number of nodes on element edges, because lower order elements are more sensitive to geometry quality around the notches.

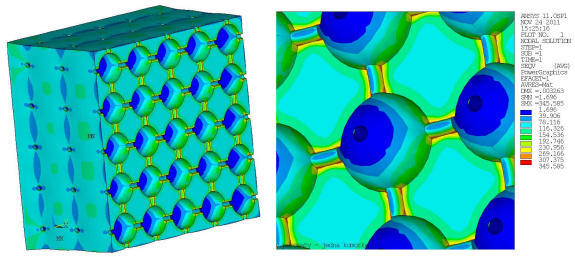

Figure 6. Typical view of stresses—section perpendicular to load direction, maximum values are near the notches—*i.e.* connection between sphere and cylindrical channel.

On the other hand, calculated displacements are nearly the same in all cases and the discrepancy is within of 0.0003 mm—it's *c.a.* 5% of average elongation which is equal 0.00625 mm. According to stiffness of the structure, dependence between Young modulus, stresses and strains

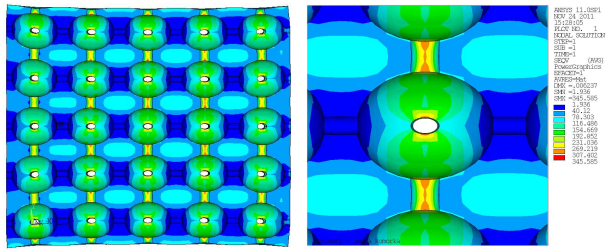

Figure 7. Typical view of stresses—section parallel to load direction.

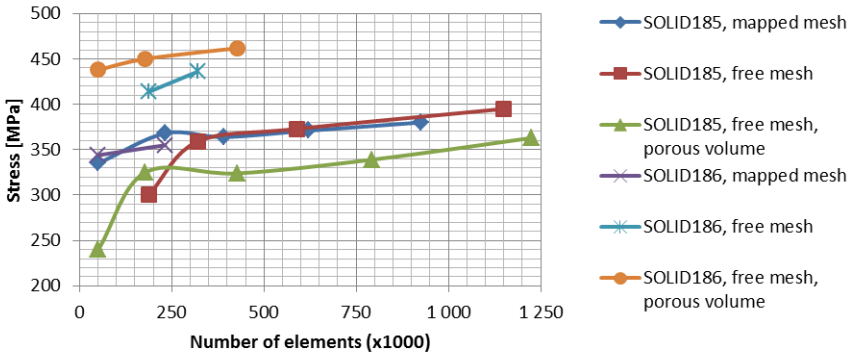

Figure 8. Variability of stresses depending on number of elements.

can be written as

$$\frac{P}{\Delta L} = E\frac{A}{L}\,,$$

where $P/\Delta L = k$ is the stiffness of scaffold, E—Young modulus, A—area of section, L—length of the scaffold. As the elongation ΔL of the scaffold is a result of the calculation, from the practical point of view it does not matter which type and shape of element will is in analysis.

CONCLUSIONS

(1) Experimental verification of mechanical properties of porous structures (designed through CAD/CAM systems and made by SLM technique) with the numerical calculations should answer the question which element type, element shapes and mesh grid gives results the most comparable to tests, while yielding acceptable calculation time.
(2) There are no distinct differences among calculated displacements in all cases both for mapped or free meshing and for low or high order elements as well.
(3) On the other hand, large differences in calculated stress were noticed for different element parameters in the same geometrical model. Range of the variation is approximately 130 MPa. However, in the case of mapped meshed models the calculated stress levels are more stable than in free meshed models.
(4) Mapped mesh in ANSYS gives more stable stress over a wide range of element set size, but its usefulness is controversial in biomedical applications because biomechanical numerical analysis are mainly based on very irregular geometries of human or animal bones and organs made with the use of CAD systems.

Table 1. Results of numerical calculations for different types, shapes and number of elements

Hexahedral volumes—Mapped mesh						
Number of elements	SOLID185		SOLID186		SOLID187	
	Stress σ [MPa]	Elongation Δl [mm]	Stress σ [MPa]	Elongation Δl [mm]	Stress σ [MPa]	Elongation Δl [mm]
50 000	335	0.00618	344	0.00631	—	—
232 000	368	0.00626	355	0.00641	—	—
390Â 000	364	0.00630	—	—	—	—
620 000	371	0.00631	—	—	—	—
925Â 000	380	0.00632	—	—	—	—
Hexahedral volumes — Free mesh						
189 000	301	0.00608	414	0.00632	414	0.00632
320 000	359	0.00624	436	0.00633	436	0.00633
590 000	373	0.00631	443	0.00633	443	0.00633
1 150 000	395	0.00636	—	—	—	—
One “porous” volume — Free mesh						
51 000	240	0.005928	438	0.00645	438	0.00645
178 000	325	0.006162	450	0.00648	450	0.00648
429 000	324	0.006252	462	0.00650	463	0.00650
792 000	339	0.006333	464	0.00650	—	—
1 226 000	363	0.006371	—	—	—	—

REFERENCES

[1] P.H. Warnke, T. Douglas, P. Wollny, E. Sherry, M. Steiner, S. Galonska, S.T. Becker, I.N. Springer, J. Wiltfang, and S. Sivananthan: *Rapid Prototyping: Porous Titanium Alloy Scaffold Produced by Selective Laser Melting for Bone Tissue Engineering*, Tissue Eng. Part C Methods **15** (2009), 115–124.

[2] R. Li, Y. Shi, Z. Wang, L. Wang, J. Liu, and W Jiang: *Densification behavior of gas and water atomized 316L stainless steel powder during selective laser melting*, Appl. Surf. Sci. **256** (2010), 4350–4356.

[3] S. Hoeges, M. Lindner, H. Fischer, W. Meiners, and K. Wissenbach: *Manufacturing of bone substitute implants using Selective Laser Melting*, IFMBE Proceedings (J.V. Sloten, P. Verdonck, M. Nyssen, and J. Haueisen, eds.), vol. 22, Springer, Berlin, 2008, pp. 2230–2234.

[4] M. Lindner, S. Hoeges, W. Meiners, K. Wissenbach, Smeets. R., R. Telle, R. Poprawe, and H. Fischer: *Manufacturing of individual biodegradable bone susbstitute implants using selective laser melting technique*, J. Biomed. Mater. Res. A **97** (2011), 466–471.

[5] F.H. Liu, R.T. Lee, W.H. Lin, and Y.S. Liao: *Selective laser sintering of bio–metal scaffold*, Procedia CIRP **5** (2013), 83–87.

[6] B. Dabrowski, W. Swieszkowski, D. Godlinski, and K. J. Kurzydlowski: *Highly porous titanium scaffolds for orthopaedic applications*, J. Biomed. Mater. Res. B Appl. Biomater. **95** (2010), 53–61.

[7] S. Deville: *Freeze–Casting of Porous Biomaterials: Structure, Properties and Opportunities*, Materials **3** (2010), 1913–1927.

[8] S.N. Dezfuli, S.K. Sadrnezhaad, M.A. Shokrgozar, and S. Bonakdar: *Fabrication of biocompatible titanium scaffolds using space holder technique*, J. Mater. Sci. Mater. Med. **23** (2010), 2483–2488.

[9] J.P. Li, J.R. Wijn, C. A. van Blitterswijk, and K. de Groot: *Comparison of Porous Ti6Al4V Made by Sponge Replication and Directly 3D Fiber Deposition and Cancellous Bone*, Key Eng. Mat. **330–332** (2007), 999–1002.

[10] C.Y. Lin, T. Wirtz, F. LaMarca, and S.J. Hollister: *Structural and mechanical evaluations of a topology optimized titanium interbody fusion cage fabricated by selective laser melting process*, J. Biomed. Mater. Res. A **83** (2007), 272–279.

[11] *ANSYS 13.0 documentation*.